α-decay properties of neutron-deficient polonium and radon nuclei

J. Wauters, P. Dendooven, M. Huyse, G. Reusen, and P. Van Duppen
Instituut voor Kern- en Stralingsfysica, Katholieke Universiteit Leuven, Celestijnenlaan 200 D, B-3001 Leuven, Belgium

P. Lievens and the ISOLDE Collaboration
CERN, CH-1211 Geneva 23, Switzerland
(Received 16 June 1992)

Chemically purified and mass-separated Rn isotopes are used to deduce the α branching ratios of the Po daughter nuclei. The obtained values are systematically lower than the previously known values. Combined with more accurate measurements of the half-lives of the neutron-deficient Po isotopes, a precise set of partial α-decay half-lives is obtained. The α-decay energies of some Po and Rn isotopes have also been remeasured. The α branching ratios of the Rn nuclei can be deduced from the α intensity of the At daughter nuclei, provided their branching is known. This makes it possible to present in a coherent way the partial α-decay half-lives and the α-reduced widths of a long chain of Po and Rn isotopes and to compare them with theory. Evidence is emerging that, for the very neutron-deficient Po isotopes, mixing of intruder configurations into the ground state is slowing down the α decay.

PACS number(s): 23.60.+e, 27.80.+w, 27.90.+b

I. INTRODUCTION

In recent years there has been renewed interest, from the experimental and theoretical sides, in the α decay of even-even nuclei. Large systematics on half-lives, α-decay energies (E_α), and α branching ratios (b_α) exist nowadays; see, e.g., [1]. For the ground state to ground state decay of even-even isotopes, with a fixed proton number Z, the partial half-lives for α decay yield striking semilogarithmic correlations with the corresponding E_α values. However, crossing a magic neutron number changes the linear relation. Based on these observations, Buck, Merchant, and Perez [2,3] were able to reproduce, in a simple cluster model with fixed parameters, the α-decay half-lives of the heavy even-even nuclei within a factor of approximately 2. They conclude that the physics in the α-decay half-lives is embedded in an α cluster having different orbitals, according to the major neutron shell, in a potential mainly governed by the available α-decay energy. This seems to contradict the Rasmussen approach [4], where the α decay is split in two parts: first the formation of the α particle, described by the reduced α width (δ^2), containing all the nuclear structure information, then followed by the tunneling of the α particle through the Coulomb and centrifugal barrier, mainly dictated by the available energy (E_α) and the change in spin. The behavior of the reduced α widths is then used to extract, out of the α decay, nuclear information such as shell closures, changes in deformation, etc. [5]. The reduced α widths of the s-wave ground state to ground state transitions between even-even nuclei are generally taken for unhindered α decay and used as a reference for the α decay in the neighboring odd-mass and odd-odd nuclei and for the α decay to excited levels.

But all of this is strongly dependent on the measured partial α-decay half-lives, thus on the total half-life and the α branching ratio. The last quantity is, in the lead region, hard to measure, as different decay channels are open and as the α branching ratio ranges from 10^{-5}% to 100%. Recently, we remeasured the α branching ratios of the neutron-deficient even Pb isotopes and compared the different ways to obtain these ratios, this in view of the longstanding problem on the α-decay half-lives of neutron-deficient Pb isotopes [6]. We also measured α-branching ratios for the neutron-deficient Fr and At isotopes [7].

Mother-to-daughter α-decay relations do not depend on the knowledge of the other decay channels. They give the most reliable α branching ratios, provided the necessary corrections are fully taken into account [8]. We have used this method to measure the α branching ratios of the Po isotopes with masses ranging from 202 down to 196. Our values are systematically 20% lower than the values given by Hornshoj *et al.* [9]. Although they also use the mother-to-daughter activity to obtain the α-branching ratio of the daughter, their values are too high due to an underestimation of the correction for recoil losses. We have also remeasured the half-lives and the α-decay energies for most of the Po isotopes. A precise set of partial α-decay half-lives, α-decay energies, and α reduced widths of the neutron-deficient Po isotopes is presented and discussed. As a by-product, we obtained also new information on the α decay of some Rn isotopes.

II. EXPERIMENTAL PROCEDURE

As discussed in Ref. [8], it is possible to precisely determine in an α-decay chain the α-branching ratio of the daughter by comparing the mother-to-daughter activity in a one-detector setup.

Mass separation of the reaction products is necessary for several reasons: the mother and daughter α lines should not only be clearly visible in the background of the other lines, but they should also be in an unique genetic relation, i.e., no direct production of the daughter nucleus may be present; implanted sources of some mm diameter implanted at a depth of typically 250 Å are excellent for high-resolution α spectroscopy; after implantation of a mass-separated beam into a tape system, the cycle time can be optimized for the half-lives of the isotopes under study.

The recoil energy of the daughter nuclei after α decay can be higher than the implantation energy of the mother nuclei. Part of the daughter nuclei can recoil out of the catcher foil, the so-called recoil losses, but these nuclei can also recoil into the detector with as a result a gain in detection efficiency. The corrections can be calculated or measured by using known decays [8].

Chemical selectivity remains in most of the cases crucial. We have been using two ways to obtain a certain chemical selectivity. At the Leuven Isotope Separator On-Line (LISOL) facility [10], an isotope separator coupled to a heavy-ion cyclotron, the selectivity of the heavy-ion fusion evaporation reaction (compound nucleus, xn versus pxn and αxn evaporation) gives some element selectivity and reduces the contamination of other masses. At the ISOLDE separator [11], chemical selectivity is obtained by the choice of the ion source and/or by the choice of the temperature of the transfer line between the target and the ion source. At the neutron-deficient side, there is, however, quite some contamination from heavier masses: the 600-MeV proton spallation reaction, used to produce the radioactivity, is rather unselective and the yield of the more stable isotopes can be orders of magnitude higher.

The precise measurements of the half-lives and α-decay energies of the $^{192-198}$Po were performed at the LISOL separator, by using the <240-MeV Ne on 2.1-mg/cm^2 ^{182}W reaction. The mass-separated beam was implanted in an aluminized mylar tape that periodically moved the source from the implantation station to a decay station or in a 30-μg/cm^2 C foil, mounted in a wheel. Silicon surface-barrier detectors and silicon PIPS-type (Passivated Implanted Planar Silicon) detectors with an active area between 50 and 450 mm^2 and an energy resolution between 11 and 20 keV for the 5.486-MeV α line of ^{241}Am were used. Energy calibration was done with online produced α emitters. In the case of short-lived nuclei, the mass-separated beam was pulsed for the half-life measurements and the growing-in and decay curve of the implanted activity was recorded by storing, in a two-parameter mode, the energy signal from the α detector and the time signal from a time to digital converter (TDC) module.

The α branching ratios of the $^{196-202}$Po isotopes were measured at the ISOLDE facility at CERN, by studying the decay of the $^{200-206}$Rn mother nuclei. The $^{200-206}$Rn isotopes were produced in the spallation reaction of a thorium-carbide target by 600-MeV protons. Chemically pure radon beams were obtained by cooling the transfer line between the thorium-carbide target and the plasma ion source. The mass-separated beam was implanted on an aluminized Mylar tape; a 25-mm^2 PIPS-type detector viewed the implantation site. The implantation periods were determined by the half-life of the Rn mother and by the production rate (in order to minimize dead-time corrections). After the implantation, the decay was followed over a long time compared to the daughter half-life, minimizing the corrections for finite counting times.

III. RESULTS

A. The Polonium isotopes

Table I gives the half-lives, α-decay energies and branching ratios of the $^{192-218}$Po isotopes from this work for $^{192-202}$Po and completed with [12] for $^{204-218}$Po. An example of a half-life measurement can be seen in Fig. 1: a fit through the 2 s growing-in and 3 s decay curve gives 0.392 (4) s for the half-life of ^{194}Po. Values for the α-decay energy (E_α) were obtained from this work, covering different experiments, and from Ref. [12]. The small errors on our values come from precise energy calibrations obtained from on-line produced activity of which the α-decay energies were known with a high accuracy (3 keV). Figure 2(a) gives a singles α spectrum at mass 206, taken at the ISOLDE separator. Three peaks are belonging to the mass 206 decay chain: the implanted activity is ^{206}Rn (6.2606 MeV), the daughter after β^+/EC (electron capture) decay is ^{206}At (5.703 MeV), the daughter after α decay is ^{202}Po (5.588 MeV). This last peak has a different shape compared to the two others. The daughter nucleus after α decay is not anymore at the same position as the mother nucleus or as the β^+/EC daughter. The α branching ratio of ^{202}Po is obtained by comparing the intensity of the ^{202}Po to the ^{206}Rn peak. The recoil correction can be calculated or experimentally determined [8]. Here we used the well-known ^{218,219,220}Rn decay chains to obtain the recoil-correction factor. The spectrum of Fig. 2(b) gives the mass 220 decay chain: the intensity of the ^{216}Po peak ($b_\alpha = 100\%$) is 1.19 (4) higher than the intensity of the ^{220}Rn peak. The α-branching ratios given in Table I were measured in this way, in one run and with the same detector at the implantation site. The tape was only moved when another mass was implanted. Our values are systematically lower than the values from Hornshoj et al. [9], who used also the mother-daughter relation (see Table I). However, they corrected only for recoil losses and not for the enhanced detection efficiency

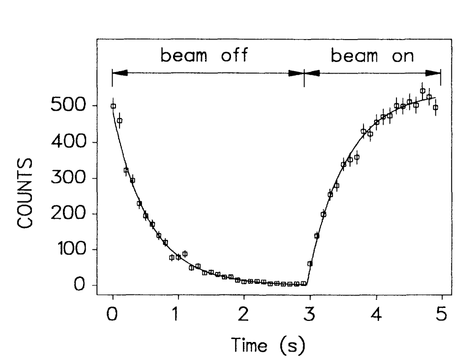

FIG. 1. TDC spectrum of the 6.842-MeV α line of ^{194}Po collected in a 2-s growing-in and 3-s decay cycle. The fit through these data points revealed a half-life of 0.392(4) s.

TABLE I. A list of obtained half-lives, α-decay energies, α branching ratios, and α reduced widths of the even-even polonium isotopes, completed with previous work. The list is extended with some results on odd-mass polonium isotopes.

Polonium	$T_{1/2}$ (s)	E_α (MeV)	b_α (%) This work	b_α (%) Other work	δ^2 (keV)
192	0.034(3)[a]	7.167(7)			68(6)[d]
193*g*	0.45(4)	6.949(5)			
193*m*	0.24(1)	7.004(5)			
194	0.392(4)	6.842(6)		93(7)[b]	70(5)
195*g*	4.64(9)	6.606(5)		63(25)[b]	
195*m*	1.92(2)	6.699(5)		73(21)[b]	
196	5.8(2)	6.521(5)	94(5)		73(5)
197*g*	53(1)	6.282(4)[a]	76(3)	90(10)[c]	
197*m*	25.8(1)	6.385(3)[a]	55(2)	~85[c]	
198	105(3)	6.180(4)	57(2)	70(8)[c]	57(3)
199*g*	312(6)[a]	5.952(2)[a]	7.5(3)	12(2)[c]	
199*m*	252(6)[a]	6.059(3)[a]	24(1)	39(4)[c]	
200	690(6)[a]	5.863(2)[a]	11.1(3)	14(2)[c]	41(12)
201*g*	918(12)[a]	5.683(2)[a]	1.10(4)	1.6(3)[c]	
201*m*	534(12)[a]	5.786(2)[a]		~3[a]	
202	2682(30)[a]	5.588(2)[a]	1.92(7)	2.2(3)[c]	36(14)
204	12708(72)[a]	5.377(1)[a]		0.66(1)[a]	30(5)
206	$7.60(9)\times10^{5}$[a]	5.2234(15)[a]		5.45(5)[a]	26(4)
208	$9.14(1)\times10^{7}$[a]	5.1158(20)[a]		100[a]	15(1)
210	$1.195\,57(1)\times10^{7}$[a]	5.304 38(12)[a]		100[a]	9.0(1)
212	$2.98(3)\times10^{-7}$[a]	8.784 37(7)[a]		100[a]	8.0(1)
214	$1.637(2)\times10^{-4}$[a]	7.686 90(6)[a]		100[a]	130(1)
216	0.150(5)[a]	6.7785(5)[a]		100[a]	150(5)
218	186.6(12)[a]	6.002 55(9)[a]		100[a]	160(2)

[a]Reference [12].
[b]Reference [19].
[c]Reference [9].
[d]The uncertainty in δ^2 only reflects the uncertainties in E_α and $T_{1/2}$; the b_α value is estimated to be 100%.

for those daughter nuclei that are implanted in the detector. Furthermore, their data taking was organized in a cycle mode with variable beam-on–beam-off periods and a movable tape collector. The daughter activity implanted in the detector is then even more important as it is not swept away by the tape: the correction for the time behavior of the daughter nuclei has to be treated separately for the activity in the tape and in the detector.

B. The Radon isotopes

Precise α-decay energies have been obtained for the $^{200-209}$Rn nuclei. Table II summarizes the results for the nuclei studied in this work completed with the data from [12] for $^{210-222}$Rn. The energy calibration was performed with on-line produced activities (^{218,219,220}Rn and ^{202}Po). At the ISOLDE separator, the cooled transfer line between the target and the ion source condensates the major part of the nonvolatile atoms. Only gaseous elements can reach the ion source. This means that in the mass 200 region the mass-separated beams consist mainly of Rn ions; At ions are suppressed to the 0.01% level, while Po ions are suppressed to the 1% level. This means that, e.g., the ^{206}At line in Fig. 2(a) is due to the β^+/EC decay of ^{206}Rn. If the α branching ratio of ^{206}At is known, the α branching ratio of ^{206}Rn can be obtained. Corrections for recoil are not necessary as the recoil energy after β^+/EC decay is very small. We could only obtain the α branching ratios of four Rn nuclei due to the fact that there is isomerism in most of the At isotopes. This was known for some odd At isotopes, but recently we studied the decay properties of neutron-deficient doubly odd At isotopes and we got evidence that for the light At, at least two isomers are α decaying. The α-branching ratios of these isomers were obtained from the mother-daughter relation after α decay of the Fr mother nucleus or from comparing the α activity of the directly produced At to the γ intensity after β^+/EC decay. The relative feeding of the different isomers can change when going from Fr α decay over direct production to the β^+/EC decay. Therefore, we cannot give values for the α branching ratios of ^{201}Rn^{m,g} and ^{203}Rn^{m,g}. In ^{204}At and ^{205}At, there is only one α-decaying state. The α-branching ratio of ^{204,205}At was measured in a separate experiment at the ISOLDE facility by studying the α decay of ^{208,209}Fr. High selectivity was obtained by using a surface ion source. The α branching ratios of ^{204,205}At were determined by comparing the mother-to-daughter activity in the same detector setup as was used for Po. The obtained values for ^{204}At and ^{205}At are, respectively, 3.8(2)% and

TABLE II. A list of obtained half-lives, α-decay energies, α branching ratios, and α reduced widths of the even-even radon isotopes, completed with previous work. The list is extended with some results on odd-mass radon isotopes.

Radon	$T_{1/2}$ (s)	E_α (MeV)	b_α (%) This work	b_α (%) Other work	δ_2 (keV)
198	0.050(9)[a]	7.196(10)[a]			200(36)[d]
199g	0.620(25)[a]	6.995(10)[a]			
199m	0.325(25)[a]	7.059(10)[a]			
200	1.06(2)[a]	6.9024(25)	86^{+14}_{-4}	~98[b]	84(14)
201	7.0(4)[b]	6.7237(25)		~80[b]	
	3.8(4)[b]	6.7721(25)		~90[b]	
202	9.85(20)[b]	6.6409(25)	80–100	85(15)[b]	77–96
203	45(3)[b]	6.4993(25)		66(9)[b]	
	28(2)[b]	6.5490(25)			
204	74.4(18)[b]	6.4189(25)	73(1)	70(2)[c]	67(19)
205	170(7)[b]	6.2609(25)	25(1)	23(2)[c]	
206	340(10)[b]	6.2606(25)		68(3)[b]	59(3)
207	558(12)[b]	6.1294(25)		35(2)[b]	
208	1461(8)[b]	6.1381(25)		60(7)[b]	39(5)
209	1710(6)[b]	6.0362(25)		17(2)[b]	
210	8640(360)[b]	6.0395(17)[b]		96(1)[b]	27(1)
212	1440(120)[b]	6.260(4)[b]		99.950(5)[b]	17(2)
214	$2.70(20)\times10^{-7}$[b]	9.037(10)[b]		100[b]	110(8)
216	$4.5(5)\times10^{-5}$[b]	8.050(10)[b]		100[b]	230(25)
218	$3.5(6)\times10^{-2}$[b]	7.1331(14)[b]		100[b]	220(38)
220	55.6(1)[b]	6.28829(10)[b]		99.93(2)[b]	240(1)
222	$3.305(1)\times10^{5}$[b]	5.4897(3)[b]		99.92[b]	240(1)

[a]Reference [20].
[b]Reference [12].
[c]Reference [9].
[d]The uncertainty in δ^2 only reflects the uncertainties in E_α and $T_{1/2}$; the b_α value is estimated to be 100%.

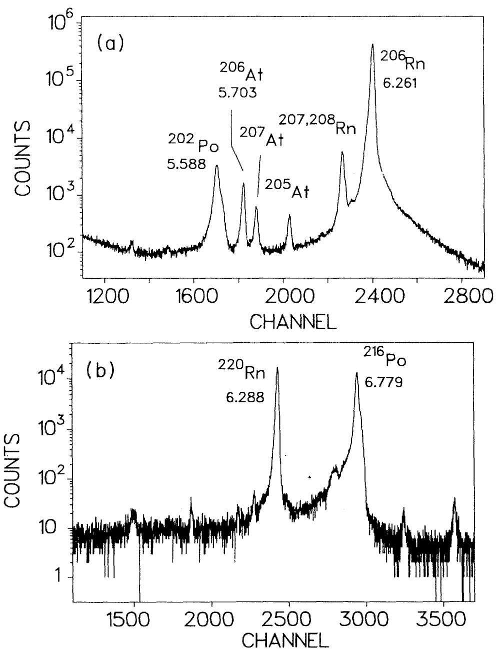

FIG. 2. (a) The singles α spectrum taken at mass 206. Energies are denoted in MeV. (b) The singles α spectrum taken at mass 220 used to determine the recoil correction factor. Energies are denoted in MeV.

9.6(4)%. The α branching ratios for ^{204,205}Rn, listed in Table II, are based on these values. The situation is more complicated for ^{202}Rn and ^{200}Rn. As discussed in Ref. [7], only one of the two known α lines of ^{202}At is seen in the pure ^{202}Rn spectrum: only the low-spin isomer of ^{202}At (184-s 6.228-MeV α line) is fed in the β^+/EC decay of ^{202}Rn. Only a lower limit on the α-branching ratio of the low-spin isomer in ^{202}At could be determined ($>13\%$) [7] resulting in $>80\%$ for the α branching ratio of ^{202}Rn. For ^{200}Rn, the α-branching ratio was determined using the α branching ratio of the 43-s low-spin isomer in ^{200}At [57(4) %] [7].

IV. DISCUSSION

Tables I and II summarize the α-decay properties of, respectively, the even-even Po and Rn isotopes. Our results are compared with the work of Hornshoj et al. [9], and are, where necessary, completed with values out of the literature. In order to have a coherent set of α-decay properties of the even-even nuclei around the $Z=82$ shell closure, we list in the Tables III–V the α-decay properties of, respectively, the platinum, mercury, and lead isotopes. Unless explicitly noted, data were taken from [12] for Pt and Hg. The results for Pb are extracted from [6]. The results for the reduced widths (δ^2) calculated with the formalism of Rasmussen [4] are included in the last

TABLE III. A list of half-lives, α-decay energies, α branching ratios, and α reduced widths of the even platinum isotopes from Ref. [12] unless stated otherwise. The b_α values for the ^{180}Pt to ^{186}Pt isotopes are estimations and are therefore questioned.

Platinum	$T_{1/2}$ (s)	E_α (MeV)	b_α (%)	δ^2 (keV)
170	$6^{+5}_{-3}\times10^{-3}$ [a]	6.548(7)	100	356(240)
172	0.105(15)	6.314(4)	94^{+6}_{-32} [b]	$130(^{+20}_{-48})$
174	0.90(1)	6.040(4)	83(5)	150(9)
176	6.33(15)	5.750(10)	41(4)	170(17)
178	21.0(7)	5.442(8)	7.2(8)	210(25)
180	52(3)	5.140(10)	(0.3)?	(110)?
182	156(6)	4.840(20)	(0.02)?	(100)?
184	1038(12)	4.490(15)	(0.001)?	(100)?
186	7200(360)	4.230(20)	(0.000 14)?	(110)?
188	$8.8(3)\times10^5$	3.919(7)	$2.6(3)\times10^{-5}$	36(4)

[a]Reference [21].
[b]Reference [22].

column of each table. Figure 3(a) shows the δ^2 values for *s*-wave ground state to ground state α decay of all known even-even nuclei ranging from Pt to No as a function of neutron number. They represent the α-decay rates excluding the probability for tunneling through the Coulomb barrier, and can be viewed as the formation probability of the α particle. The reduced widths were calculated using the α-decay energy (E_α), half-life ($T_{1/2}$), and α branching ratio (b_α) from [12] and from Tables I–V. The error bars on each point reflect the experimental error on E_α, $T_{1/2}$ and b_α.

The crucial question concerning the α reduced widths is the amount of physics that can be obtained from it. As can be seen in Fig. 3(a), the α reduced widths are lying in a range from 8 to 400 keV, but in an isotopic series the variation is quite slow, except for the $N=126$ shell gap. In a recent study on the $^{191}\text{Bi}\rightarrow{}^{187}\text{Tl}\rightarrow{}^{183}\text{Au}$ α-decay chain [13], we could not observe any influence of shape changes on the speed of α decay. Although there are strong changes from sphericity to deformation from an oblate shape to a prolate shape, the α-reduced widths are more or less constant. This was also the conclusion by Hornshoj *et al.* [14] on the basis of the reduced α-decay rates for the even thorium and radium isotopes.

Clearly, shell effects manifest themselves in large differences on the δ^2 values. At $N=126$, a sharp discontinuity is present, showing the neutron shell closure. Above $N=126$, the reduced widths increase rapidly and saturate. Below $N=126$, only a slow increase is evident. This observation can be related to the fact that in the first case, the two neutrons that constitute the α particle occupy orbits immediately above the $N=126$ shell, while below $N=126$ α decay creates two neutron holes. A second dip is visible around $N=152$, corresponding to the neutron shell closure at $N=152$. This shell effect is much weaker than at $N=126$ (for Cm there is even no dip at $N=152$), but one must bear in mind that the $N=126$ region is in fact the region of two shell closures, $N=126$ and $Z=82$, enhancing the dip in the reduced widths.

At $Z=82$, one would expect a similar shell effect: above $Z=82$ the Po and Rn isotopes should have larger reduced widths than Pb, while below $Z=82$, the Pt α decay should be faster than the Hg decay, which in turn should be somewhat faster than Pb. Except for ^{188}Pt, this is indeed the case within the experimental uncertainty.

TABLE IV. A list of half-lives, α-decay energies, α branching ratios, and α reduced widths of the even mercury isotopes from Ref. [12] unless stated otherwise.

Mercury	$T_{1/2}$ (s)	E_α (MeV)	b_α (%)	δ^2 (keV)
176	0.034^{+18}_{-9} [a]	6.767(10) [a]		61(23) [d]
178	0.260(30)	6.429(6)	(50) [b]	64(28)
180	2.56(2) [c]	6.118(15)	33(12) [a]	68(25)
182	10.84(6) [c]	5.865(15)	8.6(18)	46(10)
184	30.6(3)	5.535(15)	1.25(20)	73(12)
186	83(6)	5.094(15)	0.016(5)	60(19)
188	195(9)	4.610(20)	$3.7(8)\times10^{-5}$	41(9)

[a]Reference [22].
[b]Reference [23].
[c]Reference [24].
[d]The uncertainty in δ^2 only reflects the uncertainties in E_α and $T_{1/2}$; the b_α value is estimated to be 100%.

TABLE V. α-decay properties of the neutron-deficient even Pb isotopes, taken from Ref. [6] except for ^{210}Pb.

Lead	$T_{1/2}$ (s)	E_α (MeV)	b_α (%)	δ^2 (keV)
182	0.055^{+40}_{-35}	6.919(15)	(100)	63(46)[b]
184	0.55(6)	6.632(10)	(100)	63(7)[b]
186	4.7(1)	6.335(10)	< 100	< 97
188	25.5(1)	5.980(5)	3–10	15–51
190	72(6)	5.577(5)	0.40(4)	50(7)
192	210(6)	5.112(5)	$6.2(6)\times10^{-3}$	67(7)
194	720(30)	4.640(20)	$7.3(29)\times10^{-6}$	15(6)
210	$7.03(6)\times10^{8}$ [a]	3.720(20)[a]	$2.2(7)\times10^{-6}$ [a]	35(11)

[a]Reference [12].

[b]The uncertainty in δ^2 only reflects the uncertainties in E_α and $T_{1/2}$; the b_α value is estimated to be 100%.

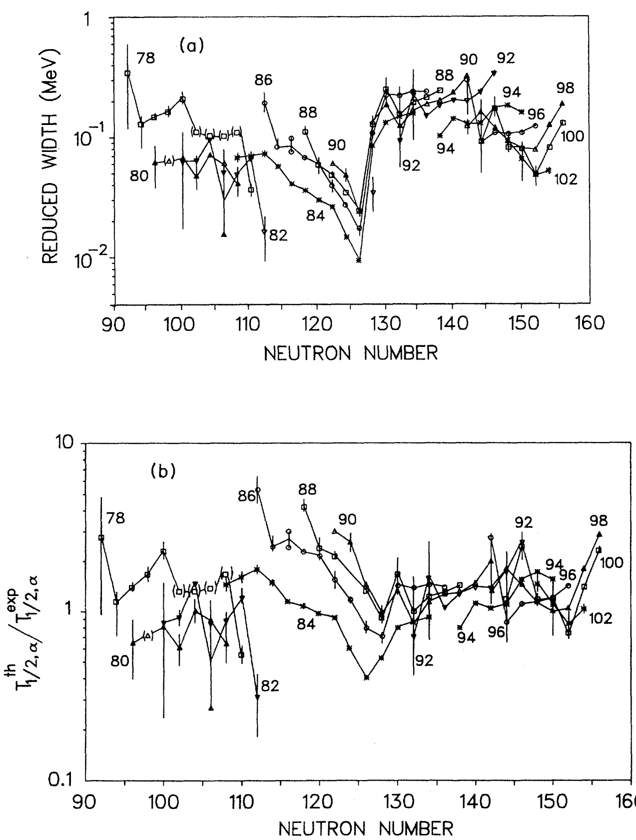

FIG. 3. (a) The reduced widths for the s-wave ground state to ground sate α decay of the even-even nuclei ranging from Pt to No, calculated with the model of Rasmussen. In two cases, only an interval can be given for δ^2, due to the α branching ratio, and is represented by a hatched region. (b) The ratios of the partial half-lives $T^{th}_{1/2,\alpha}$, calculated with the model of Buck et al., to the experimental half-lives $T^{expt}_{1/2,\alpha}$. The value for ^{210}Pb ($N=128$) is 0.10, with the principal quantum number chosen for the region $N>126$, but equals 1.37 if one decreases this quantum number with 2 units. Therefore, this nucleus is not plotted. As in (a), the hatched regions represent intervals for the plotted values due to the α branching ratio.

No evidence for a disappearance of the $Z=82$ shell closure is present, contrary to the findings of Toth et al. [5]. The Hg and Pb α decay is slower than the Pt α decay and the Pb α decay is slower than the α decay of Po and Rn. Furthermore, the existence of a shell closure at $Z=82$ is also observed in the Q_α systematics.

Recently, Buck, Merchant, and Perez published a calculation of partial α half-lives using a square well potential, correcting for neutron shell closures by using an adequate principal quantum number and excluding a formation probability [2,3]. In this way and by fitting the parameters of the model to the data set of all even-even α emitters, they are able to reproduce the partial α-decay half-life of almost all even-even α emitters within a factor of 2. They conclude that apparently no other nuclear structure information can be obtained from the partial α decay half-lives (as no formation probability was used). Figure 3(b) shows the ratios of the calculated partial half-life $T^{th}_{1/2\alpha}$ to the experimental $T^{expt}_{1/2,\alpha}$. The effect of the $N=126$ shell gap is diminished (but still present) by changing the principal quantum number. However, Fig. 3(b) still exhibits the same characteristics as Fig. 3(a). In fact, the parts in Figs. 3(a) and 3(b) below $N=126$ are identical. The model of Buck, Merchant, and Perez is based on fitting the α-decay half-lives in each major neutron shell and on a change in the principal quantum number for each neutron shell closure. This reduces the difference between the calculated and measured half-lives in two ways: first, by the fit procedure, and second, by the introduction of the neutron shell gap. However, some specific correlations in the ratio of the calculated to measured half-lives do persist. The Po, Rn, Ra, and Th values show a steep decrease when the neutron number reaches $N=126$, evidencing the influence of the neutron shell closure. Furthermore, the ratios of the calculated to experimental partial half-lives of the neutron-deficient Po, Rn, Ra, and Th isotopes are systematically increasing with increasing proton number. Again, this indicates the influence of a shell closure, here for protons. These specific correlations suggest that a formation probability cannot be excluded and that the conclusion of Buck, Merchant, and Perez that no physical structural information can be extracted from α-decay rates is too strong. To further prove our point, we will discuss in more detail the α-decay rates of the neutron-deficient Po isotopes.

For the clarity of the discussion, we come back to the conventional δ^2 plot of Fig. 3(a). The Po isotopes have δ^2 values that are systematically lower than the Rn isotopes. Furthermore, they seem to reach a saturation and even intend to decrease with decreasing neutron number around $N=110$, with δ^2 values comparable to Pb, contrary to the Rn isotopes. In ^{198}Po, we recently observed a low-lying 0^+ state that was populated in the α decay of ^{202}Rn [15]. This state has been interpreted as being the bandhead of a coexisting rotational-like band of which the 2^+ and 4^+ members were observed in an in-beam study [16]. This 0^+ state can be interpreted as a π (4p-2h) (four-particle–two-hole) intruder state. A general fingerprint of intruder states is that their excitation energies come down when approaching the midshell ($N=104$ in this case) [17]. In the case of Po, the intruder state will decrease in energy with decreasing neutron number and can mix substantially with the ground state in the lighter Po isotopes ($A \leq 196$). Indirect evidence for this effect can be found in the in-beam study of ^{196}Po [16], where the excited 2_2^+ and 4_2^+ states, believed to be the band members of the π(4p-2h) configuration, are, respectively, 180 and 95 keV lower in energy than in ^{198}Po. Although in the case of ^{198}Po little evidence for mixing between the intruder 0^+ state and the normal ground state exists [15], one can expect that the mixing will increase when the intruder state becomes lower in excitation energy. A substantial mixing of the π(4p-2h) configuration with the normal π(2p) ground-state configuration will influence the α-decay rate. The ground state of the neutron-deficient even-even Pb isotopes is rather pure, the mixing of the π(2p-2h) configuration into the ground state is small [18]: the hindered α decay of the intruder π(4p-2h) component in the ground state Po α decay to the relative pure Pb ground state will reduce the total α-decay strength of the lighter Po isotopes, giving rise to lower δ^2 values.

V. CONCLUSIONS

A precise data set of the α-decay properties of neutron-deficient Po and Rn isotopes was collected. This made it possible to deduce an accurate systematics of partial α-decay half-lives and the reduced widths of s-wave ground state to ground state α decay of even-even α emitters from Pt to Rn. No disappearance of the $Z=82$ shell closure is evident. The very-neutron-deficient Po isotopes seem to have a loss in α-decay strength, which could be due to mixing of an intruder state with the ground state in Po. Further α-decay and in-beam studies are necessary to clarify this point. Another possibility to observe the mixing of a deformed configuration into the ground state of the neutron-deficient polonium nuclei would be $\delta\langle r^2\rangle$ measurements with laser-spectroscopic methods.

ACKNOWLEDGMENTS

We want to thank J. Gentens and D. Wouters for the technical assistance at the LISOL separator and the CYCLONE cyclotron crew for the excellent beams. We are also indebted to the staff of the ISOLDE separator for their help and hospitality.

[1] B. Al-Bataina and J. Jänecke, Phys. Rev. C **37**, 1667 (1988).
[2] B. Buck, A. C. Merchant, and S. M. Perez, Phys. Rev. Lett. **65**, 2975 (1990).
[3] B. Buck, A. C. Merchant, and S. M. Perez, J. Phys. G **17**, 1223 (1991).
[4] J. O. Rasmussen, Phys. Rev. **113**, 1593 (1959).
[5] K. S. Toth, Y. A. Ellis-Akovali, C. R. Bingham, D. M. Moltz, D. C. Sousa, H. K. Carter, R. L. Mlekodaj, and E. H. Spejewski, Phys. Rev. Lett. **53**, 1623 (1984).
[6] J. Wauters, P. Dendooven, P. Decrock, M. Huyse, R. Kirchner, O. Klepper, G. Reusen, E. Roeckl, and P. Van Duppen, Z. Phys. A **342**, 277 (1992).
[7] M. Huyse, P. Decrock, P. Dendooven, G. Reusen, P. Van Duppen, and J. Wauters, Phys. Rev. C **46**, 1209 (1992).
[8] J. Wauters, P. Decrock, P. Dendooven, M. Huyse, P. Lievens, G. Reusen, and P. Van Duppen, Nucl. Instrum. Methods B **61**, 178 (1991).
[9] P. Hornshoj, K. Wilsky, P. G. Hansen, A. Lindahl, and O. B. Nielsen, Nucl. Phys. A **163**, 277 (1971).
[10] M. Huyse, P. Decrock, P. Dendooven, J. Gentens, G. Vancraeynest, P. Vandenberghe, and P. Van Duppen, Nucl. Instrum. Methods B **70**, 50 (1992).
[11] H. L. Ravn, Phys. Rep. **54**, 201 (1979); *ISOLDE User's Guide,* edited by H.-J. Kluge (CERN 86-05, Geneva, 1986).
[12] E. Browne and R. B. Firestone, *Table of Radioactive Isotopes,* edited by V. S. Shirley (Wiley, New York, 1986).
[13] J. Wauters, P. Decrock, P. Dendooven, M. Huyse, G. Reusen, and P. Van Duppen, Z. Phys. A **339**, 533 (1991).
[14] P. Hornshoj, P. G. Hansen, B. Jonson, H. L. Ravn, L. Westgaard, and O. B. Nielsen, Nucl. Phys. A **230**, 365 (1974).
[15] J. Wauters, P. Dendooven, M. Huyse, G. Reusen, P. Lievens, and P. Van Duppen, Z. Phys. A **344**, 29 (1992).
[16] D. Alber, R. Alfier, C. E. Bach, D. B. Fossan, H. Grawe, H. Kluge, M. Lach, K. H. Maier, M. Schramm, R. Schubart, M. P. Waring, L. Wood, H. Hübel, and Jing-ye Zhang, Z. Phys. A **339**, 225 (1991).
[17] J. L. Wood, K. Heyde, W. Nazarewicz, M. Huyse, and P. Van Duppen, Phys. Rep. **215**, 101 (1992).
[18] P. Dendooven, P. Decrock, M. Huyse, G. Reusen, P. Van Duppen, and J. Wauters, Phys. Lett. B **226**, 27 (1989).
[19] M. Leino, Ph.D. thesis (1983).
[20] F. Calaprice, G. T. Ewan, R.-D. von Dincklage, B. Jonson, O. C. Jonsson, and H. L. Ravn, Phys. Rev. C **30**, 1671

(1984).
[21] S. Hofmann, G. Münzenberg, F. Hessberger, W. Reisdorf, P. Armbruster, and B. Thuma, Z. Phys. A **299**, 281 (1981).
[22] J. Schneider, GSI report GSI-84-3, 1984 (unpublished).
[23] E. Hagberg, P. G. Hansen, P. Hornshoj, B. Jonson, S. Mattsson, and P. Tidemand-Petersson, Nucl. Phys. A **318**, 29 (1979).
[24] J. Wauters, P. Dendooven, M. Huyse, G. Reusen, P. Van Duppen, R. Kirchner, O. Klepper, and E. Roeckl, Z. Phys. A (in press).